PHYSICAL REVIEW B **81**, 174527 (2010)

Effect of spin-orbit coupling on the electron-phonon interaction of the superconductors Pb and Tl

R. Heid and K.-P. Bohnen
Karlsruher Institut für Technologie, Institut für Festkörperphysik, D-76021 Karlsruhe, Germany

I. Yu. Sklyadneva
Donostia International Physics Center (DIPC), P. de Manuel Lardizabal 4, 20080 San Sebastián/Donostia, Basque Country, Spain;
Institute of Strength Physics and Materials Science, pr. Academicheskii 2/1, 634021 Tomsk, Russia;
and Karlsruher Institut für Technologie, Institut für Festkörperphysik, D-76021 Karlsruhe, Germany

E. V. Chulkov
Donostia International Physics Center (DIPC), P. de Manuel Lardizabal 4, 20080 San Sebastián/Donostia, Basque Country, Spain;
Departamento de Física de Materiales, Facultad de Ciencias Químicas, UPV/EHU, Apdo. 1072, 20080 San Sebastián, Basque Country, Spain;
and Centro de Física de Materiales (CFM), Materials Physics Center (MPC), Centro Mixto CSIC-UPV/EHU, Edificio Korta, Avenida de Tolosa 72, 20018 San Sebastián, Basque Country, Spain

(Received 22 March 2010; published 24 May 2010)

The influence of spin-orbit coupling (SOC) on the electron-phonon interaction and on the pairing strength is investigated for Pb and Tl within density-functional theory. For Pb we find that SOC increases the coupling constant λ by 44%, solving the longstanding puzzle of too small λ values obtained consistently in previous first-principles calculations. The origin of the SOC-induced enhancement of λ lies both in a softening of the phonon spectrum and in an increase in the electron-phonon coupling matrix elements. In contrast, for the neighboring element Tl only weak effects of SOC on the phonon spectrum and the electron-phonon interaction is obtained, leading to an overall reduction in λ by 12%. In both cases, the inclusion of SOC improves the agreement with experiment.

DOI: 10.1103/PhysRevB.81.174527 PACS number(s): 63.20.kd, 71.15.Rf, 63.20.dk, 71.15.Mb

I. INTRODUCTION

The standard theory of phonon-mediated superconductivity, the Eliashberg theory,[1,2] provides a detailed and material-specific description of many physical properties of the superconducting state based on the knowledge of normal-state properties only, such as electronic structure, phonon spectrum, and electron-phonon interaction. In the last two decades theoretical methods based on density-functional theory (DFT) have matured to provide very reliable information about these normal-state properties for a wide range of materials. In particular, with the development of density-functional perturbation theory (DFPT), a numerically efficient approach for calculating both the phonon spectrum and the microscopic parameters of the electron-phonon interaction has been available.[3] This approach has been successful even beyond the isotropic limit of the Eliashberg theory with the multiband superconductor MgB_2 being a prominent example.[4,5] By combining with the recently developed DFT for the superconducting state, true first-principles predictions of superconducting properties are now within reach.[6,7]

For elemental superconductors, the normal-state properties are usually well captured within DFPT.[8] A prominent exception is lead, which has been the prototype of a strong-coupling superconductor since the early days of the development of the Eliashberg theory.[9,10] Pioneering tunneling experiments delivered a detailed picture of the Eliashberg coupling function and indicated a very large coupling constant of $\lambda=1.55$.[11,12] Fingerprints of strong electron-phonon coupling (EPC) are the various anomalies in the phonon dispersion observed experimentally.[13,14] Therefore, Pb has been the focus of various theoretical studies of its lattice and electron-phonon coupling properties. While a reasonable overall description of the phonon spectrum was found, it was noted early that DFT performs poorly in reproducing the various anomalies, in particular, it underestimates the deep dip at the X point in both the longitudinal and transverse branches.[8,15–18] Similar discrepancies have been obtained for EPC-related properties. With the exception of an early linear muffin-tin orbital study, which found $\lambda=1.68$,[8] more recent DFPT studies consistently underestimate the coupling, with λ ranging from 1.2 to 1.4.[16,17,19] Such large errors of more than 20% are unknown among elemental superconductors. A comparison of high-resolution measurements of phonon lifetimes of Pb with the recently developed resonant spin-echo spectroscopy also indicated that DFT largely underestimates the EPC-induced linewidths for the transverse modes.[19,20]

In view of the relatively poor performance of DFT for the phonon dispersion of Pb, it has been speculated before that it might be due to the neglect of spin-orbit coupling (SOC).[8,16] In two very resent studies, which extended the DFPT to include SOC-related effects, this conjecture has been convincingly proven to be correct.[21,22] In particular, the very detailed study of dal Corso revealed that even fine structures of the phonon dispersion related to the Fermi-surface geometry (Kohn anomalies) are well captured if SOC is taken into account.[21] The effect of SOC on the electron-phonon coupling has, however, not been considered in these studies.

In this work, we extend these studies of SOC-related effects beyond the lattice dynamics and focus, in particular, on the electron-phonon coupling properties of Pb. For that purpose we have implemented the SOC within the mixed-basis pseudopotential method. To assess the accuracy of this implementation, results for the electronic structure and phonon spectrum are presented as well, and compared with previous works. We show that SOC causes rather profound changes of the electron-phonon coupling strength in Pb and discuss their origin. In addition, we perform a similar analysis for the neighboring element Tl, whose phonon and electron-phonon coupling properties have not been studied before by *ab initio* methods.

The paper is organized as follows. The computational details are described in the following Sec. II. In Secs. III A and III B, we present results for electronic structure and phonon dispersion, respectively. The SOC effects on the electron-phonon coupling properties are discussed in detail in Sec. III C. The main findings are then briefly summarized in Sec. IV.

II. CALCULATIONAL DETAILS

The present calculations are performed in the framework of density-functional theory with the mixed basis pseudopotential approach.[23,24] The inclusion of SOC is conceptually straightforward, as the current implementation of this method employs norm-conserving pseudopotentials in a semilocal form. It has been shown by Kleinman that relativistic norm-conserving pseudopotentials can be constructed from the solution of an atomic all-electron Dirac equation, which includes relativistic effects up to second order in the fine-structure constant α.[25] The electron-ion pseudopotential in the semilocal form can then be written as[26]

$$V_{\mathrm{PS}} = \sum_l [V_l^{\mathrm{SR}}(r) + V_l^{\mathrm{SO}}(r)\mathbf{L}\cdot\mathbf{S}]\hat{P}_l, \tag{1}$$

where $\hat{P}_l$ denotes the projector onto the angular momentum channel l. Both the scalar-relativistic components $V_l^{\mathrm{SR}}(r)$ as well as the spin-orbit parts $V_l^{\mathrm{SO}}(r)$ are expressed in terms of the lj components of the pseudopotential, V_{lj}, derived from the atomic Dirac equation

$$V_l^{\mathrm{SR}}(r) = \frac{1}{2l+1}[(l+1)V_{l,l+(1/2)}(r) + lV_{l,l-(1/2)}(r)], \tag{2}$$

$$V_l^{\mathrm{SO}}(r) = \frac{2}{2l+1}[V_{l,l+(1/2)}(r) - V_{l,l-(1/2)}(r)]. \tag{3}$$

In standard scalar-relativistic calculations, the V_l^{SO} term is neglected. The implementation of SOC within other pseudopotential schemes has been described before, such as for ultrasoft pseudopotentials[27,28] and for fully separable norm-conserving pseudopotentials.[22]

The use of norm-conserving pseudopotentials can lead to fairly deep pseudopotentials, which are numerically expensive in a pure plane-wave treatment. However, they can be efficiently dealt with in the mixed-basis scheme, which employs a combination of local functions and plane waves for the representation of the valence states.[23,24] The use of local functions leads to a much faster convergence in the number of plane waves and thus reduces the size of the basis set significantly. The $V_l^{\mathrm{SO}}(r)$ term does not introduce further complications because it is short-ranged and can be treated within the mixed basis scheme in analogy to the usual short-ranged semilocal part of V_l^{SR}.

Phonon- and electron-phonon coupling properties are calculated using the linear response technique or DFPT (Ref. 3) in combination with the mixed-basis pseudopotential method.[29] As these calculations involve first and second derivatives of the Kohn-Sham Hamiltonian with respect to atomic displacements, similar first and second derivatives of V_l^{SO} are required. They are additive to the scalar-relativistic pseudopotential contributions and can be treated in analogy to the derivatives of the short-ranged semilocal parts of V_l^{SR}.

For both Pb and Tl, norm-conserving pseudopotentials were constructed following the description of Vanderbilt.[30] We have compared pseudopotentials with and without $5d$ semicore state included. While for Pb the differences both in electronic and phononic properties were marginal, we observed a larger difference for Tl. Therefore, throughout the present study we used pseudopotentials with the semicore $5d$ states treated explicitely as valence states. To treat the deep d potentials, we used $5d$-type local functions at each atomic site supplemented by plane waves up to a kinetic energy of 20 Ry. The local-density approximation (LDA) in the parameterization of Hedin-Lundqvist[31] was applied for the exchange-correlation functional. Brillouin-zone (BZ) integrations were performed by k-point sampling in conjunction with the standard smearing technique[32] employing a Gaussian broadening of 0.2 eV. For the phonon calculations we used a $16\times16\times16$ fcc k-point mesh for Pb and a $24\times24\times16$ hexagonal mesh for Tl, corresponding to 408 and 488 k points in the irreducible BZ (IBZ). For the calculations of electron-phonon coupling matrix elements, denser meshes of $32\times32\times32$ (2992 points in IBZ) and $36\times36\times24$ (1524 points in IBZ) for Pb and Tl, respectively, were required to obtain sufficient convergence of the slowly converging Fermi-surface averages.

III. RESULTS AND DISCUSSION

A. Geometry and electronic structure

The results for the lattice optimizations are summarized in Table I. The equilibrium lattice constants and bulk moduli are obtained by a fit of the total energy as a function of volume to the Murnaghan equation of state.[34] For hcp Tl, the total energy for each given volume is found by minimizing the energy with respect to the c/a ratio. The results for Pb both with and without SOC are in very good agreement with the LDA study by Dal Corso.[21] The inclusion of the SOC leads only to a marginal increase in a and a slight softening of the bulk modulus by 4%. The SOC effects are opposite in the case of Tl, where a shrinks by 0.7% and the bulk modulus hardens by 3.5%.

The electronic band structures for the optimized geometries are shown in Fig. 1. The modifications due to SOC are consistent with those found in previous studies of Pb (Refs.

TABLE I. Calculated lattice constants and Bulk moduli of fcc-Pb and hcp-Tl.

		a (a.u.)	c/a	B (Mbar)
Pb (fcc)	Without SOC	9.229		0.519
	With SOC	9.243		0.497
	Expt.[a]	9.269		0.49
Tl (hcp)	Without SOC	6.459	1.588	0.420
	With SOC	6.417	1.601	0.435
	Expt.[b]	6.496	1.593	

[a]Reference 18.
[b]Reference 33.

22 and 35) and of Tl,[36,37] respectively. The most significant changes for Pb occur in the vicinity of the zone-boundary point W, which however have very little effect on the shape of the Fermi surface.[21] In the case of Tl, SOC changes the Fermi-surface topology, as it leads to a splitting of bands right at Fermi energy E_F in the $k_z=0$ plane. Nevertheless, the SOC produces only minor modifications in the electronic density of states (DOS) (see right panels in Fig. 1). For Pb,

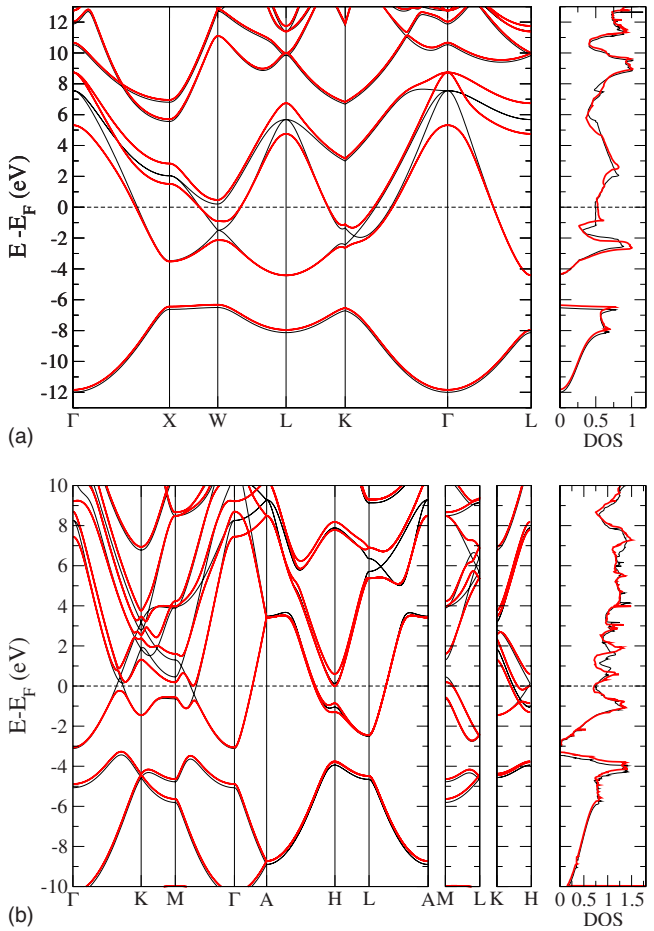

FIG. 1. (Color online) Electronic band structure of Pb and Tl calculated for the optimized structures. The thin (black) lines denote semirelativistic calculations while the thick (red) lines include spin-orbit interaction.

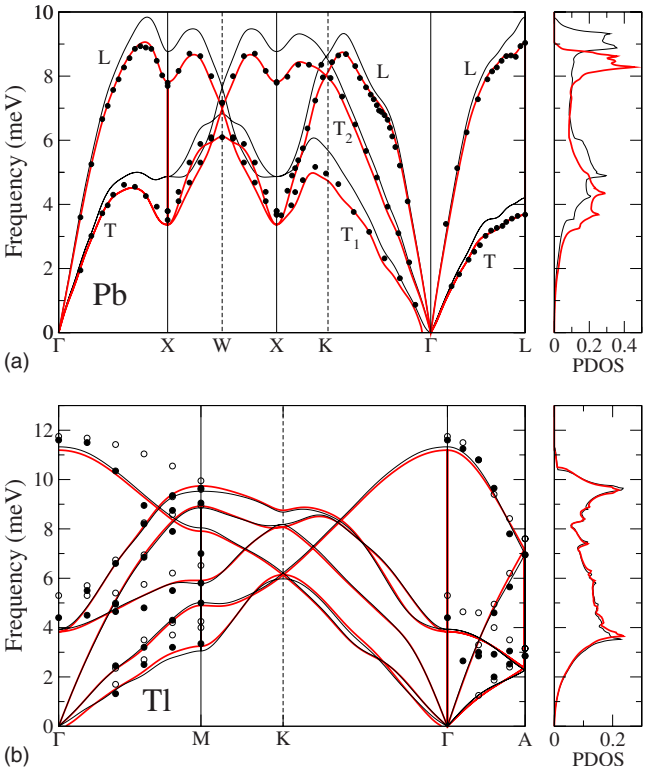

FIG. 2. (Color online) Phonon dispersions and phonon density of states of Pb and Tl. Thick (red) lines represent calculations including SOC and thin (black) lines those without SOC. Experimental data for Pb (filled circles) are taken from Ref. 13 ($T=100$ K) and Ref. 14 (data along XWX, $T=80$ K). For Tl, data are taken from Ref. 38 (filled symbols: $T=297$ K, open symbols: $T=77$ K).

the SOC increases the DOS at E_F by 6% [from 0.491 to 0.520 states/(eV unit cell)] while for Tl the introduction of small band splittings leads to a decrease in $N(E_F)$ by 5% [from 0.802 to 0.762 states/(eV unit cell)].

B. Phonon dispersion

In Fig. 2, the phonon dispersions of Pb and Tl calculated both with and without SOC are compared to experimental data. For Pb, the SOC induces a softening of practically all branches despite the fact that the optimized lattice constants are almost the same. As can be inferred for the phonon DOS shown in Fig. 2, the average softening is about 15% for the transverse modes, and only about 8% for the longitudinal ones. SOC improves the agreement with the experimental dispersion in various aspects, most prominent for the anomaly in the transverse branch at X. Our results are in very good quantitative agreement with the recent LDA calculation by Dal Corso,[21] who also showed in detail that the SOC leads to an improved description of the Kohn anomalies along the [110] and [111] directions.

In the case of Tl, the effect of SOC on the phonon spectrum is much more subtle. SOC-induced frequency changes are smaller than 0.2 meV, resulting in an almost identical phonon DOS. To our knowledge, the only measurements of the phonon dispersion of Tl has been performed by Worlton and Schmunk[38] at two different temperatures. Their data are

also plotted in Fig. 2. They found surprisingly large differences between room temperature and 77 K but also reported large error bars for the measured frequencies. Our DFPT results are in reasonable agreement with the room-temperature data with the exception of the TO branch along Γ-A. Data taken at 77 K suggest an unusally pronounced hardening of many branches with decreasing temperature. They are in clear discrepancy with the DFPT results, which should correspond to the limit $T \to 0$. This issue will be addressed further in Sec. III C.

C. Electron-phonon coupling and superconductivity

In the following we will address the effect of SOC on the electron-phonon coupling focusing first on Pb. The Eliashberg function relevant for an isotropic s-wave superconductor can be expressed as

$$\alpha^2 F(\omega) = \frac{1}{2\pi\hbar N(E_F)} \sum_{\mathbf{q}\lambda} \frac{\gamma_{\mathbf{q}\lambda}}{\omega_{\mathbf{q}\lambda}} \delta(\omega - \omega_{\mathbf{q}\lambda}), \tag{4}$$

where $N(E_F)$ is the electronic density of states (per atom and spin) at the Fermi energy, $\omega_{\mathbf{q}\lambda}$ denotes the frequency of the phonon mode $(\mathbf{q}\lambda)$, and $\gamma_{\mathbf{q}\lambda}$ is defined as

$$\gamma_{\mathbf{q}\lambda} = 2\pi\omega_{\mathbf{q}\lambda} \sum_{\mathbf{k}\nu\nu'} |g^{\mathbf{q}\lambda}_{\mathbf{k}+\mathbf{q}\nu',\mathbf{k}\nu}|^2 \delta(\epsilon_{\mathbf{k}\nu} - E_F) \delta(\epsilon_{\mathbf{k}+\mathbf{q}\nu'} - E_F). \tag{5}$$

Here, $\epsilon_{\mathbf{k}\nu}$ are the one-electron band energies with momentum $\mathbf{k}$ and band index ν, and g denotes the screened EPC matrix element and is given by

$$g^{\mathbf{q}\lambda}_{\mathbf{k}+\mathbf{q}\nu',\mathbf{k}\nu} = \sqrt{\frac{\hbar}{2\omega_{\mathbf{q}\lambda}}} \sum_{\kappa a} \frac{1}{\sqrt{M_\kappa}} \eta^{\mathbf{q}\lambda}_{\kappa a} \langle \mathbf{k}+\mathbf{q}\nu' | \delta^{\mathbf{q}}_{\kappa a} V | \mathbf{k}\nu \rangle \tag{6}$$

M_κ is the mass of the κth atom in the unit cell and $\eta^{\mathbf{q}\lambda}_{\kappa a}$ is the normalized eigenvector of the phonon mode $(\mathbf{q}\lambda)$. $\delta^{\mathbf{q}}_{\kappa a} V$ denotes the first-order change in the total crystal potential with respect to the displacement of the atom κ in the a direction. It consists of the change in the screening potential (Hartree and exchange correlation) and in the pseudopotential

$$\delta V = \delta V_{\mathrm{scr}} + \delta V_{\mathrm{PS}} = \delta V_{\mathrm{scr}} + \delta V_{\mathrm{SR}} + \delta V_{\mathrm{SO}} \tag{7}$$

and thus contains a contribution from the change in the SOC potential.

As shown by Allen,[39] $\gamma_{\mathbf{q}\lambda}$ can be approximately interpreted as the contribution to the phonon linewidth (half width at half maximum) coming from electron-phonon interaction in the limit $T \to 0$. Because g contains a factor $\omega^{-1/2}_{\mathbf{q}\lambda}$, $\gamma_{\mathbf{q}\lambda}$ does not depend on the phonon frequencies. In Fig. 3, $\gamma_{\mathbf{q}\lambda}$ is shown for phonons along high-symmetry directions calculated both with and without SOC. The inclusion of SOC leads to enhancements of $\gamma_{\mathbf{q}\lambda}$ over large parts of the BZ, which is particularly pronounced for the transverse branch along [100] and for T_1 along [110]. At the X point, its value is almost doubled. We note, that despite these SOC-induced enhancements, there is no indication of a peak in $\gamma_{\mathbf{q}\lambda}$ of the T_1 branch along $(\xi\xi 0)$ near $\xi = 0.35$, as has been observed in a recent resonant spin-echo spectroscopy study.[19]

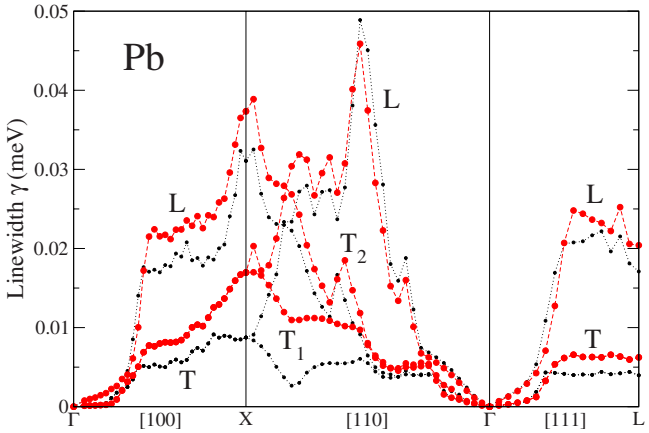

FIG. 3. (Color online) Calculated phonon linewidths (half widths at half maximum) on a dense mesh along high-symmetry lines for Pb. Thick (red) circles denote results obtained with SOC and thin (black) circles those without SOC.

SOC also affects $\gamma_{\mathbf{q}\lambda}$ of the longitudinal modes with the largest linewidth increases found for the L branch along [100]. In contrast to this general trend, the large peak in $\gamma_{\mathbf{q}\lambda}$ for the longitudinal branch along [110], which is well known to be related to a Fermi-surface nesting,[13] is slightly reduced by the SOC.

The effect of SOC on the Eliashberg function is shown in Fig. 4. On the one hand, it results in a shift of the transverse and longitudinal peaks to lower frequencies due to the softening of the phonon spectrum. On the other hand, the weights of the peaks are also significantly enhanced. Comparison with $\alpha^2 F$ extracted from tunneling measurements (open circles in Fig. 4) shows a dramatic improvement by taking into account the SOC in describing both the position and the height of the main spectral features.

The average electron-phonon coupling constant is related to the Eliashberg function by

$$\lambda = 2\int_0^\infty d\omega \frac{\alpha^2 F(\omega)}{\omega} = \frac{1}{\pi\hbar N(E_F)} \sum_{\mathbf{q}\lambda} \frac{\gamma_{\mathbf{q}\lambda}}{\omega^2_{\mathbf{q}\lambda}}. \tag{8}$$

Both the shift to lower frequencies and the increased weight of the peaks in $\alpha^2 F$ promote an increase in λ. Without SOC we obtained $\lambda = 1.08$, which is slightly smaller than those of previous studies, presumably because of a somewhat harder phonon spectrum. With inclusion of SOC, λ increases by 44% to 1.56, which then agrees nicely with the experimental value of 1.55.[12]

λ depends essentially on three different quantities: (i) the phonon frequencies, (ii) the number of electronic states at the Fermi surface available for scattering processes, as represented by the product of δ functions in Eq. (5), and (iii) the EPC matrix elements. According to Eq. (8), λ should scale approximately as $1/\omega^2$, because $\gamma_{\mathbf{q}\lambda}$ does not depend on the phonon frequencies. To estimate the importance of the phonon softening, we have evaluated the formulas above using electronic states and EPC matrix elements from the calculation without SOC and combining it with the phonon spectrum from the calculation including SOC. Then λ increases

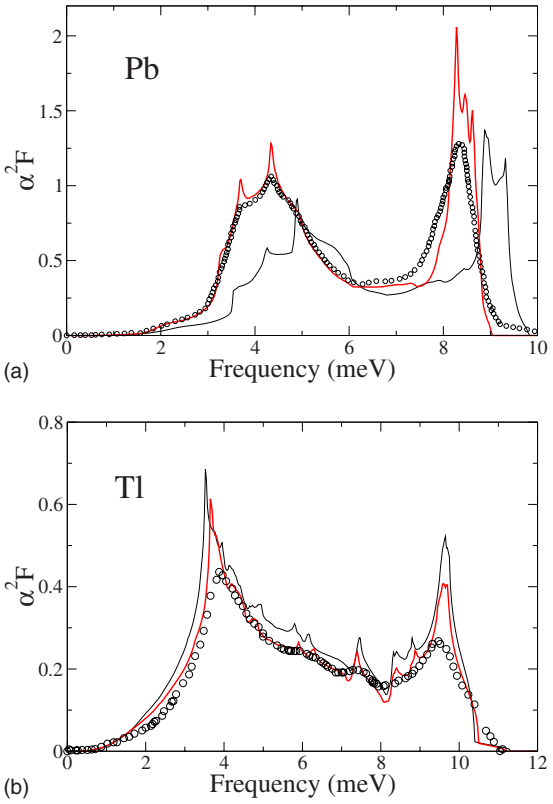

FIG. 4. (Color online) Eliashberg functions of Pb and Tl. Thick (red) and thin (black) lines are calculations with and without SOC, respectively. Open circles denote results from tunneling experiments taken from Refs. 11 and 40 for Pb and Tl, respectively.

from 1.08 to 1.33 (22%). Thus, the softening of the phonon spectrum due to SOC accounts for approximately half of the increase of λ. An estimate for the effect of (ii) is obtained by noting that λ scales approximately with the density of states at E_F, which amounts to only a 6% increase due to SOC. Consequently, there must be an additional increase in λ coming from an enhancement of the EPC matrix elements themselves. To check this directly, we have calculated λ by taking all electronic and phononic quantities from the SOC calculation but setting $\delta V_{SO}=0$ in the evaluation of the EPC matrix elements [see Eqs. (6) and (7)]. Indeed this reduces λ from 1.56 to 1.35 (decrease of 14%).

In stark contrast to the large influence of SOC on the EPC properties of Pb, the coupling strength of Tl is slightly weakened when SOC is taken into account. λ is reduced from 1.00 to 0.87 (12%), as indicated by minor modifications in α^2F (Fig. 4). The SOC-induced changes improve the agreement with experiment although still λ is overestimated as compared to the experimental value of 0.795.[12] The fact that the shape of the calculated α^2F does reproduce the experimental one in many details argues in favor of the correct theoretical description of the underlying phonon spectrum. Comparison with the measurements by Worlton and Schmunk[38] suggests that their room-temperature data represent the proper phonon spectrum of Tl but that the low-temperature data might contain serious errors.

IV. SUMMARY

We have studied the influence of spin-orbit interaction on the electron-phonon coupling in two elemental superconductors, Pb and Tl. These neighboring elements in the periodic table have in common that they are both *sp*-type metals with similar density of states at the Fermi energy (per atom) and are both strong-coupling superconductors ($\lambda \approx 0.87-1.55$). Despite these similarities they exhibit quite different behavior when SOC is taken into account. For Pb, the phonon spectrum softens significantly which improves the agreement with measured dispersion curves, as has been found previously.[21,22] In addition, we found a large enhancement of the coupling strength by 44%, which partly reflects the strong SOC-induced softening, but also has a significant contribution from the SOC-related increase in the electron-phonon coupling matrix elements. In contrast, the lattice dynamics of Tl exhibits only a weak influence of SOC and the total coupling strength is slightly reduced by 12%. For both Pb and Tl, with the inclusion of SOC, the calculated Eliashberg functions are now in excellent agreement with those extracted for tunneling experiments.

[1] G. M. Eliashberg, Zh. Eksp. Teor. Fiz. **38**, 966 (1960) [Sov. Phys. JETP **11**, 696 (1960)].
[2] D. J. Scalapino, in *Superconductivity*, edited by R. D. Parks (Marcel Dekker, New York, 1969), Vol. 1.
[3] S. Baroni, S. de Gironcoli, and A. Dal Corso, Rev. Mod. Phys. **73**, 515 (2001).
[4] A. Y. Liu, I. I. Mazin, and J. Kortus, Phys. Rev. Lett. **87**, 087005 (2001).
[5] H. J. Choi, D. Roundy, H. Sun, M. L. Cohen, and S. G. Louie, Phys. Rev. B **66**, 020513(R) (2002).
[6] M. Lüders, M. A. L. Marques, N. N. Lathiotakis, A. Floris, G. Profeta, L. Fast, A. Continenza, S. Massidda, and E. K. U. Gross, Phys. Rev. B **72**, 024545 (2005).
[7] M. A. L. Marques, M. Lüders, N. N. Lathiotakis, G. Profeta, A. Floris, L. Fast, A. Continenza, E. K. U. Gross, and S. Massidda, Phys. Rev. B **72**, 024546 (2005).
[8] S. Y. Savrasov and D. Y. Savrasov, Phys. Rev. B **54**, 16487 (1996).
[9] J. R. Schrieffer, D. J. Scalapino, and J. W. Wilkins, Phys. Rev. Lett. **10**, 336 (1963).
[10] D. J. Scalapino, J. R. Schrieffer, and J. W. Wilkins, Phys. Rev. **148**, 263 (1966).
[11] W. L. McMillan and J. M. Rowell, in *Superconductivity*, edited by R. D. Parks (Marcel Dekker, New York, 1969), Vol. 1.
[12] R. C. Dynes and J. M. Rowell, Phys. Rev. B **11**, 1884 (1975).
[13] B. N. Brockhouse, T. Arase, G. Cagliotti, K. R. Rao, and A. D. B. Woods, Phys. Rev. **128**, 1099 (1962).
[14] R. Stedman, L. Almqvist, and G. Nilsson, Phys. Rev. **162**, 549 (1967).
[15] S. de Gironcoli, Phys. Rev. B **51**, 6773 (1995).

[16] A. Y. Liu and A. A. Quong, Phys. Rev. B **53**, R7575 (1996).
[17] A. Floris, A. Sanna, S. Massidda, and E. K. U. Gross, Phys. Rev. B **75**, 054508 (2007).
[18] B. Grabowski, T. Hickel, and J. Neugebauer, Phys. Rev. B **76**, 024309 (2007).
[19] P. Aynajian, T. Keller, L. Boeri, S. M. Shapiro, K. Habicht, and B. Keimer, Science **319**, 1509 (2008).
[20] T. Keller, P. Aynajian, K. Habicht, L. Boeri, S. K. Bose, and B. Keimer, Phys. Rev. Lett. **96**, 225501 (2006).
[21] A. Dal Corso, J. Phys.: Condens. Matter **20**, 445202 (2008).
[22] M. J. Verstraete, M. Torrent, F. Jollet, G. Zérah, and X. Gonze, Phys. Rev. B **78**, 045119 (2008).
[23] S. G. Louie, K.-M. Ho, and M. L. Cohen, Phys. Rev. B **19**, 1774 (1979).
[24] B. Meyer, C. Elsässer, F. Lechermann, and M. Fähnle, *FORTRAN90 Program for Mixed-Basis-Pseudopotential Calculations for Crystals* (Max-Planck-Institut für Metallforschung, Stuttgart).
[25] L. Kleinman, Phys. Rev. B **21**, 2630 (1980).
[26] G. B. Bachelet and M. Schlüter, Phys. Rev. B **25**, 2103 (1982).
[27] A. Dal Corso and A. Mosca Conte, Phys. Rev. B **71**, 115106 (2005).
[28] A. Dal Corso, Phys. Rev. B **76**, 054308 (2007).
[29] R. Heid and K.-P. Bohnen, Phys. Rev. B **60**, R3709 (1999).
[30] D. Vanderbilt, Phys. Rev. B **32**, 8412 (1985).
[31] L. Hedin and B. J. Lundqvist, J. Phys. C **4**, 2064 (1971).
[32] C.-L. Fu and K. M. Ho, Phys. Rev. B **28**, 5480 (1983).
[33] C. S. Barrett, Phys. Rev. **110**, 1071 (1958).
[34] F. D. Murnaghan, Proc. Natl. Acad. Sci. U.S.A. **30**, 244 (1944).
[35] K. Horn, B. Reihl, A. Zartner, D. E. Eastman, K. Hermann, and J. Noffke, Phys. Rev. B **30**, 1711 (1984) and references therein.
[36] M. A. E. A. Ament and A. R. de Vroomen, J. Phys. F: Met. Phys. **7**, 97 (1977).
[37] P. M. Holtham, J.-P. Jan, and H. L. Skriver, J. Phys. F: Met. Phys. **7**, 635 (1977).
[38] T. G. Worlton and R. E. Schmunk, Phys. Rev. B **3**, 4115 (1971).
[39] P. B. Allen, Phys. Rev. B **6**, 2577 (1972).
[40] R. C. Dynes, Phys. Rev. B **2**, 644 (1970).